Polymer 53 (2012) 3211–3219

Contents lists available at SciVerse ScienceDirect

Polymer

journal homepage: www.elsevier.com/locate/polymer

# Free radical polymerization of ethyl methacrylate and ethyl α-hydroxy methacrylate: A computational approach to the propagation kinetics

Berna Dogan [a], Saron Catak [b], Veronique Van Speybroeck [b], Michel Waroquier [b], Viktorya Aviyente [a,*]

[a] Department of Chemistry, Boğaziçi University, 34342 Bebek, İstanbul, Turkey
[b] Center for Molecular Modeling, Ghent University-Member of the QCMM-Alliance Ghent-Brussels, Technologiepark 903, 9052 Zwijnaarde, Belgium

ARTICLE INFO

*Article history:*
Received 7 March 2012
Received in revised form
8 May 2012
Accepted 10 May 2012
Available online 29 May 2012

*Keywords:*
Free radical polymerization
Modeling
Solvent effect

ABSTRACT

The propagation kinetics of ethyl methacrylate (EMA) and ethyl α-hydroxy methacrylate (EHMA) has been subject to a computational study to understand their free radical polymerization (FRP) behavior in bulk and in solution using Density Functional Theory (DFT). The propagation of EHMA is studied in ethanol and toluene to assess the effect of hydrogen-bonding solvents on FRP of monomers with α-hydroxy functionality. Although EMA and EHMA resemble each other in structure, EHMA propagates faster in bulk due to the presence of intermolecular hydrogen-bonds, which tend to facilitate the approach of the propagating species. This falls in contrast with the experimentally observed lower propagation rates of EHMA in ethanol compared to toluene. Calculations show that the 2.28 rate acceleration in toluene is governed by the ratio of the pre-exponential factors, which reflect the entropies of activation, in both media. The polar protic solvent ethanol has a disruptive effect via hydrogen-bonding on the 6-membered ring shape of EHMA monomers thus decreasing the entropy of activation of the reaction. In the case of toluene, there are no special interactions with the hydrophobic solvent, the entropy of activation is higher than in ethanol.



## 1. Introduction

Free radical polymerization (FRP) is one of the most widely used reactions, since it enables the synthesis of high molecular weight polymers from a variety of monomers [1]. Due to its wide applicability, understanding the mechanism of FRP has become a common goal for both experimentalists and theoreticians [2]. Acrylates and methacrylates are among the most commonly used monomers in FRP. They can be used as dental materials, biomaterials, adhesives, optical adhesives, coatings, fiber-optic coatings, aspherical lenses for CD applications, contact lenses and photolithography [3]. Recently, hydroxy-functional acrylic and methacrylate monomers have been studied both experimentally and theoretically [4–9] due to their hydrophilicity, crosslinking sites and functionality for subsequent reactions.

It is known that ester derivatives of α-hydroxy methacrylates – RHMA's – show fast photopolymerization rates both on their own and in the presence of acrylate or methacrylate crosslinkers [10]. The ester group's effect on the free radical polymerization of α-hydroxymethacrylates has been theoretically investigated [8b] and the polymerization rate was shown to be correlated to the steric hindrance caused by the alkyl substituents. More specifically, the bulky alkyl group in *t*-butyl α-hydroxymethacrylates (TBHMA) was suggested to inhibit propagation when compared to the smaller alkyl groups in ethyl α-hydroxymethacrylates (EHMA) and methyl α-hydroxymethacrylates (MHMA) and the trend in $k_p$'s for α-hydroxymethacrylates was calculated as: $k_p(\text{MHMA}) > k_p(\text{EHMA}) > k_p(\text{TBHMA})$ [7a]. Furthermore, in the case of MHMA, a rate enhancing effect of the intermolecular hydrogen-bonding between propagating radicals was reported [8b].

In recent years, there is an increased interest in the development of bioactive polymeric dental composites and related materials that have potential for mineralized tissue regeneration and preservation. Ethyl α-hydroxy methacrylate (EHMA) is known to have acceptable ion releasing properties and is considered a suitable substitute for 2-hydroxy methacrylate (HEMA), a structural isomer of EHMA, in dental and possibly biomedical applications due to its smaller water affinity [11]. Random copolymerization of EHMA with styrene and methacrylate yields polymers that have potential applications as biomaterials [12]. Furthermore, EHMA can be utilized in catalytic chain transfer polymerization – an effective technique to control the molecular weight in FRP [13].

Due to the potential bio-applicability, the polymerization behavior of EHMA has been subject to several experimental studies.

* Corresponding author.
*E-mail address:* aviye@boun.edu.tr (V. Aviyente).

0032-3861/$ – see front matter © 2012 Elsevier Ltd. All rights reserved.
doi:10.1016/j.polymer.2012.05.018

Davis *et al.* have used Pulsed Laser Polymerization (PLP) technique to measure the propagation rate constant ($k_p$) of EHMA in different solvents; however, due to catalytic chain transfer, $k_p$ of EHMA in bulk was not successfully measured [5]. However, the variation of $k_p$ in different solvents was found to be substantially larger than that previously observed for any other acrylic or styrenic monomer. On the other hand, the polymerization behavior of ethyl methacrylate (EMA) – a monomer extensively used in the contact lens industry due to its ease of polymerization with radical initiators [14] – was successfully studied by Zammit *et al.* by PLP in bulk [4]. The comparison of propagation rate constants of the two polymers shows that EHMA $k_p$ values are 12–40% times higher than those for EMA [4,5]. Higher $k_p$ values for EHMA are actually surprising, since the hydroxymethyl group is bulkier than the methyl group; it is suggested that this is caused by the hydroxyl group's electronic influence on the radical center and/or on the EHMA monomer reactivity. Similarly, Ueda *et al.* [9a] have reported that introducing heteroatoms into the methyl group increases the reactivity of these monomers due to inductive effects. Nevertheless, the effect of hydrogen-bonding on polymerization kinetics should also be taken into consideration, since EHMA is prone to intermolecular hydrogen-bonding through its hydroxyl group (Scheme 1). Many experimental studies report that monomers with hydrogen-bonding capability have higher polymerization rates compared to their non-hydrogen-bonding analogs [15]. In fact Hoyle *et al.* [15b] have shown by FTIR that hydrogen-bonds are present during hydroxyalkyl acrylate polymerization and the rate is directly related with hydrogen-bond formation. This increase in polymerization rate is attributed to both the increase in propagation rate and the decrease in termination rate.

Recently, the effect of solvent on the free radical polymerization kinetics, conversion and regularity has been studied [6,16,17]. Beuermann *et al.*, particularly emphasized the influence of organic solvents on the propagation rates of monomers with hydroxy functionality [17]. It was concluded that in the case of non-hydrogen-bonding solvents – solvents that cannot form hydrogen-bonds with the monomer or the macromolecular species – the relative size of the solvent as compared to the monomer governs whether $k_p$ will be higher or lower than its value in bulk. It is shown that effect of solvent (ones that are not able to form hydrogen-bonds) is higher when the sizes of monomer and solvent are far different than each other; and the effect is lower almost nonexistent if the sizes of monomer and solvent are close to each other. For hydrogen-bonding solvents, which can form hydrogen-bonds with the monomer or the propagating radical, the effect of H-bonding on reactivity should be explicitly considered.

Davis *et al.* [5] have monitored the free radical polymerization kinetics of EHMA in three different solvents, namely, toluene, tetrahydrofuran (THF) and ethanol. It was found that in the case of ethanol and THF (polar solvents with hydrogen-bonding capacity), $k_p$ decreases upon increased solvent ratios, whereas an increase in $k_p$ is observed when the amount of toluene (non-hydrogen-bonding hydrophobic solvent) was increased (Table 1). These findings have been attributed to special interactions between the solvent and the propagating species in the case of ethanol and THF.

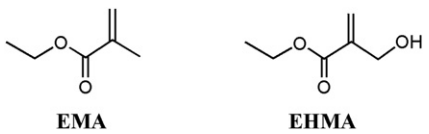


**Scheme 1.** Structures of ethyl methacrylate (EMA) and ethyl α-hydroxymethacrylate (EHMA).

Herein, the propagation reaction of EMA and EHMA is subject to a computational study in order to understand their polymerization behavior and the effect of the α-hydroxy functionality. Moreover, hydrogen-bonding modes of EHMA – intramolecular and intermolecular– and their effect on the propagation kinetics will be thoroughly investigated both in bulk and in solution. For this purpose, a hydrogen-bonding solvent, ethanol and a hydrophobic solvent, toluene, have been chosen and results are rationalized based on the experimental data of Davis *et al.* [5].

## 2. Computational details

Density Functional Theory (DFT) with the Gaussian 03 [18] program package is used for gas phase calculations. For calculations in solution, the Gaussian 09 [19] program package is used, since it provides significantly enhanced solvation features. Geometry optimizations are carried out with B3LYP/6-31 + G(d) [20] for all monomers, radicals and transition states. Harmonic vibrational frequencies were computed at the same level of theory and used to provide thermal corrections to the Gibbs free energies, and to confirm the nature of the stationary points. DFT functionals BMK [21] and MPW1K [22] have been employed for energy refinement. BMK (Becke-Martin for kinetics), a hybrid meta GGA model, is considered to be a reliable general-purpose functional whose capabilities have been expanded to cover transition states [21]. MPW1K, also a hybrid Hartree-Fock-density functional (HF-DF), reduces the mean unsigned error in reaction barrier heights by a factor of 2.40 and predicts barrier heights more accurately than other widely used methods [22].

The conventional transition state theory (TST) [23] is used to calculate the rate constant for the bimolecular reaction as follow:

$$k_2 = \kappa \frac{kT}{h} \frac{RT}{p^{\theta}} e^{\frac{-\Delta G^{\ddagger}}{RT}}$$

in this equation $k$ represents Boltzmann's constant, $T$ is the temperature, $h$ is Planck's constant, $\Delta G^{\ddagger}$ represents the Gibbs free energy difference between the activated complex and the reactants, $R$ is the universal gas constant, $\kappa$ is the transmission coefficient which is assumed to be about 1 and $p^{\theta}$ is the standard pressure $10^5$ Pa (1 bar).

The reaction kinetics of EMA and EHMA are compared initially in the gas phase and then by using a dielectric continuum model, namely, the integral equation formalism model (IEF-PCM) [24] with UFF radii. In continuum solvation models, the solvent is represented as a polarizable medium characterized by its static dielectric constant $\varepsilon$ and the solute is embedded in a cavity surrounded by this dielectric medium [25]. For calculations in bulk, the dielectric constant of EMA has been replaced by the one of methyl methacrylate (MMA) ($\varepsilon = 3.00$) based on the lack of information on the former and the similarity of EMA to MMA. Due to the lack of experimental information the dielectric constant of EHMA has been taken as 7.80, which is the dielectric constant of methyl α-hydroxy methacrylate (MHMA). The effect of the solvent on the free radical polymerization kinetics of EHMA was calculated by employing both an implicit (toluene and ethanol) and a mixed implicit/explicit [26] solvation model (for ethanol only). Implicit models which include additional terms for the nonelectrostatic contributions of the solvent, such as dispersion, repulsion, and cavitation, are generally thought to be reliable only when explicit solute–solvent interactions (e.g., hydrogen-bonds) are not present. Since EHMA, is capable of hydrogen-bonding with ethanol, the solvent effect with ethanol has been considered explicitly. On the other hand, the effect of non-hydrogen-bonding solvents like toluene has been

**Table 1**
Kinetic parameters for EMA [4] and EHMA [5] obtained from experiment. Activation energies ($E_a$), pre-exponential constants ($A$) obtained in the temperature range 283–313 K; propagation rate constants ($k_p$) at 303 K for EHMA and at 301 K for EMA.

| Monomer | Monomer / Solvent (w/w) | Monomer / Solvent (n/n) | $E_a$ (kcal mol$^{-1}$) | $A$ ($10^6$ L mol$^{-1}$ s$^{-1}$) | $k_p$ (L mol$^{-1}$ s$^{-1}$) | Relative $k_p$ (L mol$^{-1}$ s$^{-1}$) |
|---|---|---|---|---|---|---|
| EHMA | Toluene 3:1 | Toluene 1:0.47 | 3.85 | 0.84 | 1331 | 1.52 |
| | Toluene 1:1 | Toluene 1:1.41 | 4.80 | 4.50 | 1496 | 1.71 |
| | Toluene 1:3 | Toluene 1:4.24 | 4.73 | 5.47 | 2098 | 2.40 |
| | Ethanol 3:1 | Ethanol 1:0.94 | 3.49 | 0.34 | 1047 | 1.20 |
| | Ethanol 1:1 | Ethanol 1:2.82 | 4.95 | 3.64 | 950 | 1.09 |
| | Ethanol 1:3 | Ethanol 1:8.47 | 4.95 | 3.27 | 875 | 1.00 |
| EMA | Bulk | | 5.71 | 4.45 | 307 | 0.35 |

taken into account with continuum solvation models due to the lack of explicit interactions between the solute and the solvent.

Corrections for basis set superposition errors (BSSE) [27], were calculated at each level of theory. Gibbs free energies of activation are calculated as the sum of the electronic energy, the thermal corrections to Gibbs free energy and the BSSE correction. In solution, the free energy of activation is calculated as the sum of electronic energies in solution, thermal correction to Gibbs free energy from gas phase, BSSE correction from gas phase and also a correction term, $RT$ ln (24.46), to take into account the conversion from 1 mol L$^{-1}$ (gas) to 1 mol L$^{-1}$ (solution) [28]. Energies reported are in kcal mol$^{-1}$, propagation rate constants ($k_p$) are in L mol$^{-1}$ s$^{-1}$. All calculations were done at 303 K.

Rotational potential energy scans around the forming bond are performed in order to locate the energetically most stable transition states [29]. The weighted average of the Gibbs free energies of activation, $\langle \Delta G^{\ddagger} \rangle$, were calculated by taking into account the Boltzmann distribution (shown below) of each state (each transition state) for EHMA and EMA both in gas phase and in solution.

$$\langle \Delta G^{\ddagger} \rangle = \sum_{i=1}^{n} \Delta G_i^{\ddagger} \left( \frac{N_i}{N_T} \right)$$

where $\frac{N_i}{N_T} = e^{-\Delta(\Delta G_i^{\ddagger})/RT} \Big/ \sum_{i=1}^{n} e^{-\Delta(\Delta G_i^{\ddagger})/RT}$ and $\Delta G_i^{\ddagger}$ is the Gibbs free energy of activation of the $i$th state and $\Delta(\Delta G_i^{\ddagger})$ is the difference between the Gibbs free energy of activation of the $i$th state and the most populated (most stable) state.

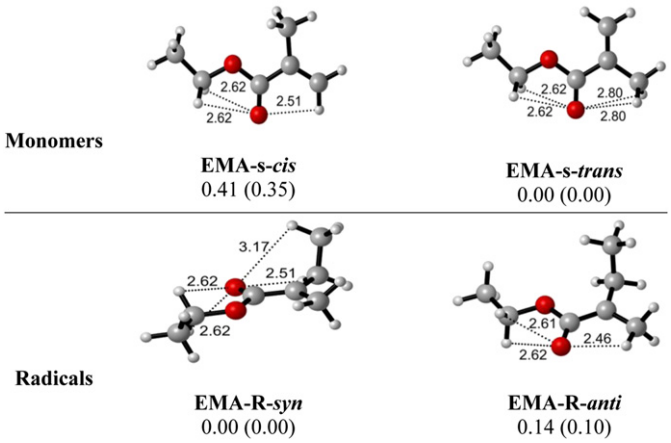


**Fig. 1.** Structures and relative Gibbs free energies of the EMA monomer and radical, EMA-R. IEF-PCM ($\varepsilon$ = 3.00 for EMA bulk) calculations in parenthesis. MPW1K/6-311 + G(3df,2p)//B3LYP/6-31 + G(d).

## 3. Results and discussion

Both syndiotactic and isotactic dimeric chains were used to study the propagation step in the FRP of EMA and EHMA. Ethanol and toluene were used as solvents in modeling the polymerization of EHMA.

### 3.1. Propagation of EMA

Based on a conformational analysis carried out for EMA (Fig. 1), the *trans* monomer and the *syn* radical of EMA are found to be slightly more stable than their counterparts. The *trans* conformer of methyl methacrylate, MMA, is shown to be more favorable due to long range interactions between the methyl group and the carbonyl group of the monomer [7b]. Similarly, in EMA four H atoms interact with the carbonyl oxygen in the *trans* conformer, however, only three such interactions are present in the *cis* conformer, so the *trans* conformer is slightly more stabilized. In the EMA radical, EMA-R, the difference between relative energies is even smaller. Since the stabilizing interactions of the carbonyl oxygen atom are almost identical, there is only a weak interaction between the oxygen atom and the ethyl H-atom in the *syn* conformer, which is absent in the *anti* conformer, this makes the *syn* conformer slightly more stable (Fig. 1).

The radical's direction of attack is of utmost importance because it determines the tacticity of the polymer chain: isotactic, syndiotactic or atactic. In Scheme 2, the *syn* radical's four different attack modes to the s-*cis* and the s-*trans* monomers are shown; with the inclusion of the *anti* radical, eight different attack conformations have been located for EMA (Table 2, Fig. 2).

Transition state structures are shown in Fig. 2 along with relative Gibbs free energies. The critical distances in all transition structures are similar. **TS-EMA-1**, **TS-EMA-2, TS-EMA-5** and **TS-EMA-6** are stabilized by interactions between the carbonyl

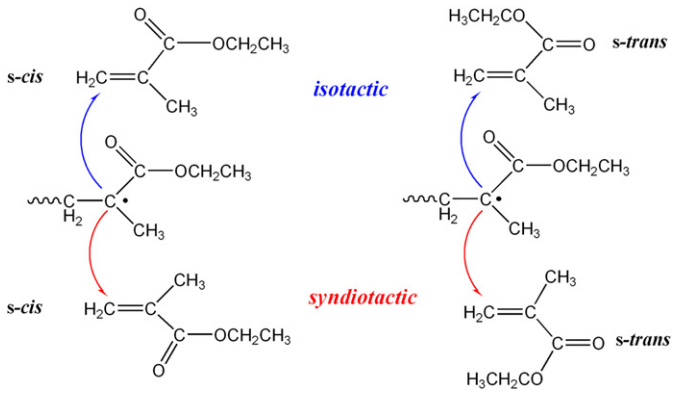


**Scheme 2.** *Syn* radical addition to s-*cis* and s-*trans* **EMA**.

**Table 2**
Gibbs free energies of activation (kcal mol$^{-1}$) of EMA at 303 K.[a,b]

| | Tacticity | Monomer | Radical | $\Delta G^{\ddagger}$ | |
|---|---|---|---|---|---|
| | | | | BMK[c] | MPW1K[d] |
| TS-EMA-1 | syndiotactic | *cis* | *anti* | 21.14 (19.85) | 21.59 (20.30) |
| TS-EMA-2 | syndiotactic | *cis* | *syn* | 20.89 (19.74) | 21.78 (20.63) |
| TS-EMA-3 | syndiotactic | *trans* | *anti* | 21.90 (20.34) | 22.32 (20.76) |
| TS-EMA-4 | syndiotactic | *trans* | *syn* | 21.89 (20.40) | 22.10 (20.61) |
| *Weighted Average* | syndiotactic | | | 21.15 (19.95) | 21.80 (20.53) |
| TS-EMA-5 | isotactic | *cis* | *anti* | 20.98 (19.77) | 21.81 (20.60) |
| TS-EMA-6 | isotactic | *cis* | *syn* | 21.09 (19.86) | 21.55 (20.33) |
| TS-EMA-7 | isotactic | *trans* | *anti* | 21.87 (20.32) | 22.24 (20.69) |
| TS-EMA-8 | isotactic | *trans* | *syn* | 21.54 (20.07) | 22.03 (20.56) |
| *Weighted Average* | isotactic | | | 21.19 (19.94) | 21.79 (20.52) |
| *Weighted Average* | Overall | | | 21.17 (19.94) | 21.80 (20.52) |

[a] BSSE corrections included.
[b] IEF-PCM ($\varepsilon = 3.00$ for bulk EMA) calculations in parenthesis.
[c] BMK/6-311 + G(3df,2p)//B3LYP/6-31 + G(d).
[d] MPW1K/6-311 + G(3df,2p)//B3LYP/6-31 + G(d).

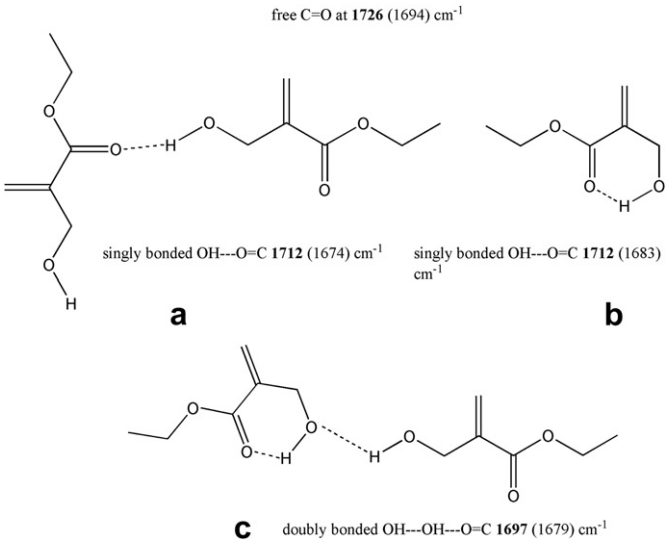


**Scheme 3.** Hydrogen-bonding modes in the EHMA monomer monitored by Infra-Red (IR) Spectroscopy in bold [11]; computed harmonic frequencies (B3LYP/6-31 + G(d)) are shown in parenthesis.

oxygen and alkyl group hydrogens. These structures are slightly more stable than the ones which do not have the latter stabilizing interactions. Since the same monomer and radical (**EMA-anti** and **EMA-R-syn**) are used in all calculations, the activation energies in Table 2 depict the relative stabilities of the transition structures, which are very close in energy to each other. The average $\Delta G^{\ddagger}$ is calculated by using the Boltzmann weighted average formula; both functionals yield similar results. In addition, experimental evidence suggests that in EMA polymerization stereoregularity is syndiotactic [30].

### 3.2. Propagation of EHMA

In the case of EHMA (analogous to MHMA) the *trans* monomer with a hydrogen-bond between the hydroxyl group and the carbonyl oxygen is the most stable conformer as expected and shown by Degirmenci *et al.* [7b]. The structure of bulk EHMA has been analyzed by Antonucci *et al.* [11] who claim that EHMA forms a 6-membered ring structure via intramolecular H-bonding (Scheme 3). Infra-red (IR) spectroscopy of EHMA shows that the carbonyl stretching peak occurred at a lower wavenumber (1712 cm$^{-1}$) than that of monomers which bear a carbonyl group, such as HEMA (1719 cm$^{-1}$). The lower wavenumber (longer bond) for EHMA is an indication that hydrogen-bonding is stronger overall. Harmonic frequencies computed for several hydrogen-bonding modes of EHMA were compared to experimental IR wavenumbers [11] (Scheme 3). Computed harmonic frequencies were scaled by a factor of 0.9636 to account for the finite basis set employed, as well as the neglect of anharmonic effects and electron correlation [31]. In line with experimental findings, intermolecular hydrogen-bonding clearly reduces the computed carbonyl wavenumber (1674 cm$^{-1}$ and 1679 cm$^{-1}$ in Scheme 3a and c, respectively) as compared to the computed wavenumber for free carbonyl (1694 cm$^{-1}$, for free carbonyl in **EHMA-3**, Fig. 3). Calculations show

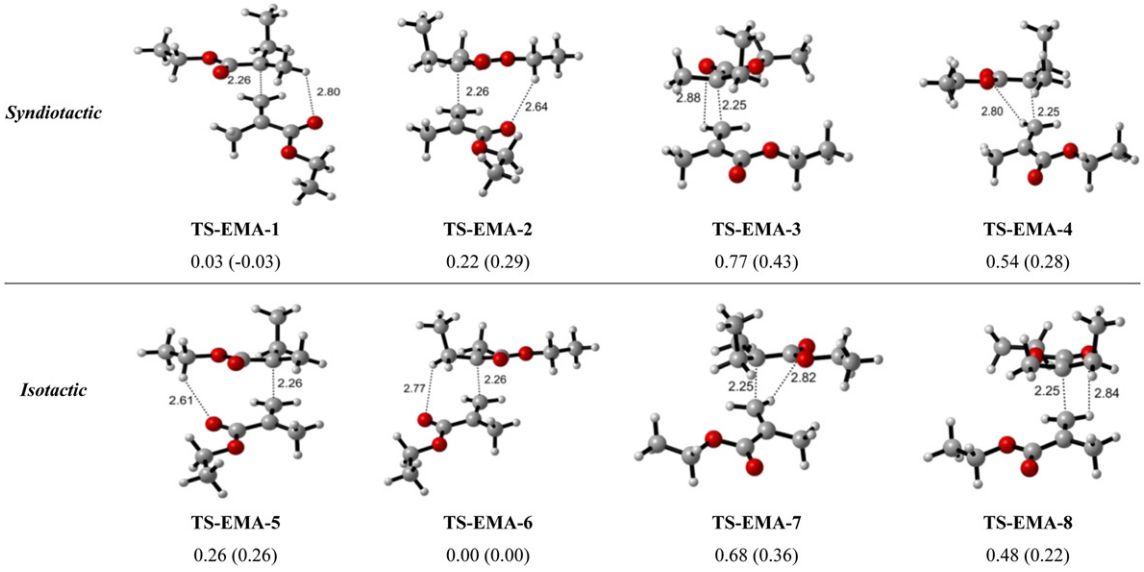


**Fig. 2.** Structures and relative Gibbs free energies (BSSE corrections included) of the transition states of EMA. IEF-PCM ($\varepsilon = 3.00$ for bulk EMA) calculations in parenthesis. MPW1K/6-311 + G(3df,2p)//B3LYP/6-31 + G(d).

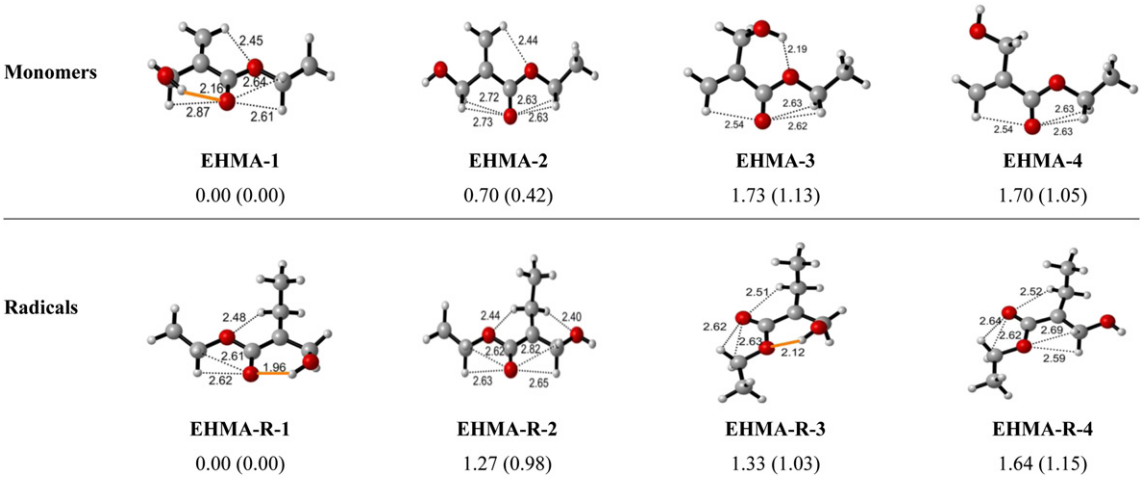


**Fig. 3.** Structures and relative Gibbs free energies of monomers and radicals of EHMA. IEF-PCM ($\varepsilon = 7.80$ for bulk EHMA) calculations in parenthesis. MPW1K/6-311 + G(3df,2p)//B3LYP/6-31 + G(d). Orange bonds show intramolecular H-bonds. (For interpretation of the references to color in this figure legend, the reader is referred to the web version of this article.)

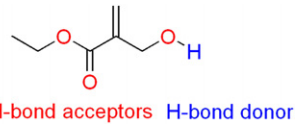


**Scheme 4.** Hydrogen-bond donor and acceptor atoms in the EHMA monomer.

that intermolecular hydrogen-bonding has a larger effect than intramolecular.

Note that EHMA is both a hydrogen-bond acceptor and donor (Scheme 4). Not only can EHMA form intramolecular hydrogen-bonds, but it can also form intermolecular ones as reported by Antonucci *et al.* [11]. Thus, there are several modes of hydrogen-bonding within and among the monomer and radical, which have been thoroughly considered (Table 3, Fig. 4). The results indicate that addition of the *anti* radical (**EHMA-R-1** and **EHMA-R-2**) to the *trans* (**EHMA-1** and **EHMA-2**) and *cis* monomers (**EHMA-3** and **EHMA-4**) are favored over the other transition structures. When the *anti* radical attacks the *cis* monomer, hydrogen-bonds are formed between the carbonyl and the hydroxyl group as in **TS-EHMA-1**. In general, syndiotactic transition structures are shown to be more stable, except for **TS-EHMA-6**, which is stabilized by intermolecular hydrogen-bonds.

The attack of the *anti* radical (**EHMA-R-2**) to the *cis* monomer (**EHMA-2**) is most favored for syndiotactic addition, hence **TS-EHMA-1** – with two intermolecular hydrogen-bonds (1.93 Å and 1.87 Å)– is more stable than the others. For the isotactic addition, attack of the *syn* radical (**EHMA-R-2**) to the *cis* monomer (**EHMA-2**) is preferred, hence, **TS-EHMA-6** with two intermolecular hydrogen-bonds (2.01 Å and 2.04 Å) is the most favorable. Structures of all calculated transition states are shown in Fig. 4. Here, the stability differences between transition states are more pronounced compared to those of EMA (Fig. 3). The second energetically favored transition state after **TS-EHMA-1** is **TS-EHMA-2** which is also an intermolecular hydrogen-bonded transition state. Moreover, transition states with intramolecular hydrogen-bonds (**TS-EHMA-3, TS-EHMA-5** and **TS-EHMA-7**) are less favored. Transition states with one intramolecular and one intermolecular hydrogen-bond (**TS-EHMA-4** and **TS-EHMA-8**) are the least favorable; this could be due to the less stable *syn* radical.

Beuermann *et al.* [6] have explained the free radical polymerization behavior of hydroxypropyl methacrylate HPMA and suggested that the hydrogen-bonds that are already present

**Table 3**
Gibbs free energies of activation (kcal mol$^{-1}$) for EHMA at 303 K.[a,b]

| | Tacticity | M | R | H-bonding | $\Delta G^{\ddagger}$ | |
|---|---|---|---|---|---|---|
| | | | | | BMK[c] | MPW1K[d] |
| TS-EHMA-1 | syndiotactic | *cis* | *anti* | MOH-RCO ROH-MCO | 17.49 (17.16) | 19.28 (18.93) |
| TS-EHMA-2 | syndiotactic | *cis* | *syn* | MOH-RCO ROH-RCO | 17.96 (18.17) | 19.72 (19.92) |
| TS-EHMA-3 | syndiotactic | *trans* | *anti* | MOH-MCO ROH-RCO | 19.22 (19.51) | 20.69 (20.98) |
| TS-EHMA-4 | syndiotactic | *trans* | *syn* | MOH-MCO ROH-MEtO | 21.02 (20.37) | 22.23 (21.57) |
| Weighted average | syndiotactic | | | | 17.70 (17.37) | 19.52 (19.17) |
| TS-EHMA-5 | isotactic | *cis* | *anti* | MOH-MEtO ROH-RCO | 21.09 (20.56) | 22.35 (21.82) |
| TS-EHMA-6 | isotactic | *cis* | *syn* | MOH-RCO ROH-MCO | 18.25 (18.19) | 20.32 (20.24) |
| TS-EHMA-7 | isotactic | *trans* | *anti* | MOH-MCO ROH-RCO | 21.50 (20.90) | 21.90 (21.31) |
| TS-EHMA-8 | isotactic | *trans* | *syn* | MOH-RCO ROH-REtO | 21.04 (20.27) | 22.58 (21.81) |
| Weighted average | isotactic | | | | 18.32 (18.33) | 20.53 (20.56) |
| *Weighted average* | | | | | 17.80 (17.50) | 19.63 (19.32) |

M: monomer; R: radical; MOH: monomer hydroxyl; ROH: radical hydroxyl; MCO: monomer carbonyl; RCO: radical carbonyl; MEtO: monomer ethoxy; REtO: radical ethoxy.
[a] BSSE corrections included.
[b] IEF-PCM calculations ($\varepsilon = 7.80$ for bulk EHMA) in parenthesis.
[c] BMK/6-311 + G(3df,2p)//B3LYP/6-31 + G(d).
[d] MPW1K/6-311 + G(3df,2p)//B3LYP/6-31 + G(d).

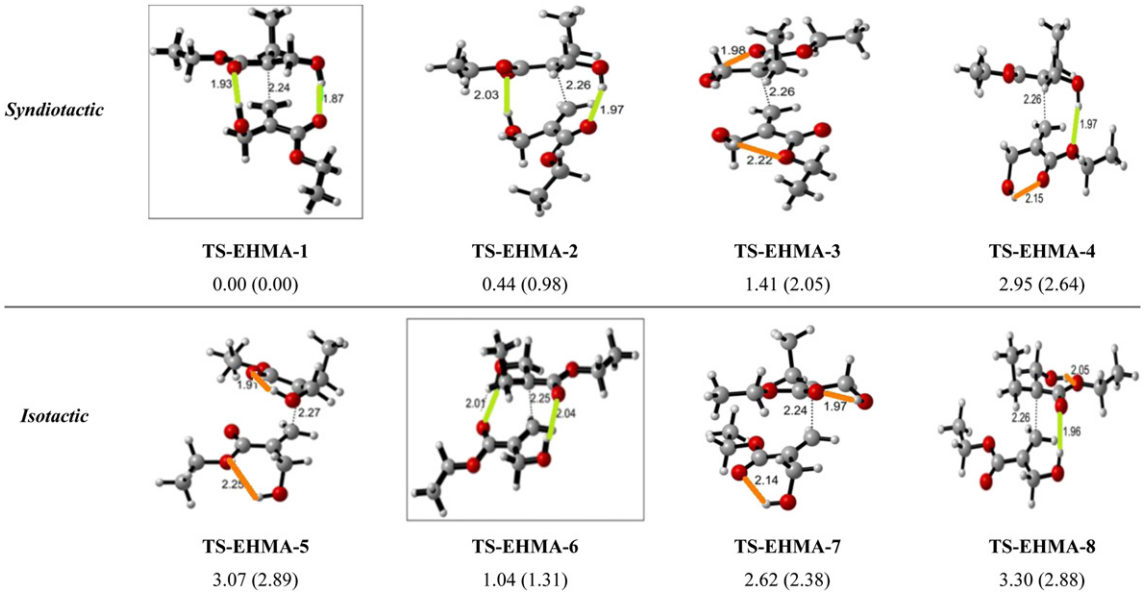


**Fig. 4.** Structures and relative Gibbs free energies (BSSE corrections included) of the transition states of EHMA. IEF-PCM ($\varepsilon$ = 7.80 for bulk EHMA) calculations in parenthesis. MPW1K/6-311 + G(3df,2p)//B3LYP/6-31 + G(d). Orange bonds show intramolecular H-bonds, green bonds show intermolecular H-bonds. (For interpretation of the references to color in this figure legend, the reader is referred to the web version of this article.)

**Table 4**
Weighted averages of Gibbs free energies of activation (kcal mol$^{-1}$) and propagation rate constants (L mol$^{-1}$ s$^{-1}$) for EMA and EHMA.[a,b]

| | | EMA | EHMA | $k_{p\ (EMA/EHMA)}$[e] |
|---|---|---|---|---|
| BMK[c] | $\Delta G^{\ddagger}$ | 21.17 (19.94) | 17.80 (17.50) | 0.004 (0.017) |
| | $k_p$ | 0.09 (0.66) | 22.99 (37.76) | |
| MPW1K[d] | $\Delta G^{\ddagger}$ | 21.80 (20.52) | 19.63 (19.32) | 0.027 (0.135) |
| | $k_p$ | 0.03 (0.25) | 1.10 (1.86) | |

[a] BSSE corrections included.
[b] IEF-PCM calculations ($\varepsilon$ = 3.00 for bulk EMA, $\varepsilon$ = 7.80 for bulk EHMA) in parenthesis.
[c] BMK/6-311 + G(3df,2p)//B3LYP/6-31 + G(d).
[d] MPW1K/6-311 + G(3df,2p)//B3LYP/6-31 + G(d).
[e] The predicted experimental $k_{p(EMA)}/k_{p(EHMA)}$ ratio as explained in text is 0.35.

between the monomer molecules shift between monomers and macromolecules during the polymerization. This statement supports our findings in a way that the transition states of EHMA with intermolecular hydrogen-bonds are more stable than those with intramolecular hydrogen-bonds. Degirmenci *et al.* [7b] also studied the propagation behavior of EHMA in gas phase, taking into account intermolecular hydrogen-bonding possibilities between the monomer and radical; they have reported that transition states with intramolecular hydrogen-bonds (**TS-EHMA-3**, Fig. 4 in this paper) are energetically more favorable compared to intermolecular hydrogen-bonded transition states. However, they only considered the possible attacks of the most stable radical to the most stable monomer; herein all possible combinations are considered as shown in Scheme 2. The current study shows that hydrogen-bonds between the monomer carbonyl and the radical hydroxyl significantly stabilizes the transition state and this conformation is only possible if the monomer is *cis* instead of the more stable conformation, *trans*. Overall the intermolecular hydrogen-bonded transition state (e.g.**TS-EHMA-1,** Fig. 4) is found to be energetically more favorable than the intramolecular hydrogen-bonded transition states e.g. **TS-EHMA-3**. Additionally, Davis *et al.* [5] have claimed that the interactions between the monomer and propagating radical in the transition state may cause a tacticity preference in EHMA polymerization, in line with our results based on Gibbs free energy differences, which show that the free radical polymerization of **EHMA** is 85% syndiotatic.

**Table 5**
Gibbs free energies of activation (kcal mol$^{-1}$) and propagation rate constants (L mol$^{-1}$ s$^{-1}$) from explicit/implicit solvent calculations for EHMA in ethanol and toluene at 303 K.[a]

| | BMK[b] | | MPW1K[c] | |
|---|---|---|---|---|
| | $\Delta G^{\ddagger}$ | $k_p$ | $\Delta G^{\ddagger}$ | $k_p$ |
| TS-EHMA-1 (implicit toluene) | 16.58 | 175.23 | 18.22 | 11.54 |
| TS-EHMA-1 (implicit ethanol) | 17.31 | 51.65 | 19.08 | 2.76 |
| TS-EHMA-1-r1 | 19.15 (16.42) | 2.47 (229.62) | 18.78 (18.25) | 4.50 (10.97) |
| TS-EHMA-1-r2 | 19.21 (17.17) | 2.23 (65.90) | 18.93 (18.79) | 3.51 (4.47) |
| TS-EHMA-1-m1 | 16.25 (18.07) | 300.67 (14.70) | 16.48 (19.85) | 207.22 (0.76) |
| TS-EHMA-1-m2 | 16.98 (17.24) | 90.13 (58.57) | 17.80 (19.28) | 22.97 (1.97) |
| TS-EHMA-1-b1 | 16.74 (17.59) | 135.11 (32.78) | 17.08 (19.67) | 75.70 (1.03) |
| TS-EHMA-1-b2 | 17.87 (18.22) | 20.58 (11.56) | 18.31 (19.92) | 9.94 (0.68) |
| *Weighted average* | 16.57 (16.91) | 176.96 (101.24) | 16.83 (18.72) | 115.49 (5.03) |

[a] IEF-PCM calculations ($\varepsilon$ = 24.85 for ethanol) in parenthesis.
[b] BMK/6-311 + G(3df,2p)//B3LYP/6-31 + G(d).
[c] MPW1K/6-311 + G(3df,2p)//B3LYP/6-31 + G(d).

**Table 6**
Ratio $k_{p(toluene)/(ethanol)}$ of rate constants for EHMA in toluene and ethanol at 303 K.

| | | BMK[a] | MPW1K[b] | Experimental[c] |
|---|---|---|---|---|
| $k_{p\ (toluene)}/k_{p\ (ethanol)}$ | $Toluene_{imp}/Ethanol_{imp}$[d] | 3.39 | 4.16 | 2.40 |
| | $Toluene_{imp}/Ethanol_{exp\text{-}imp}$[e] | 1.73 | 2.28 | |

[a] BMK/6-311 + G(3df,2p)//B3LYP/6-31 + G(d).
[b] MPW1K/6-311 + G(3df,2p)//B3LYP/6-31 + G(d).
[c] Rate constants are taken from reference 4 and 5 and reproduced in Table 1.
[d] For $Toluene_{imp}/Ethanol_{imp}$: **TS-EHMA-1** in continuum is considered for both toluene and ethanol (Table 5, first two rows).
[e] $Toluene_{imp}/Ethanol_{exp\text{-}imp}$: **TS-EHMA-1** in continuum is considered for toluene; for ethanol the weighted average of the explicit-implicit solvent model is considered (Table 5, last row, values in parenthesis).

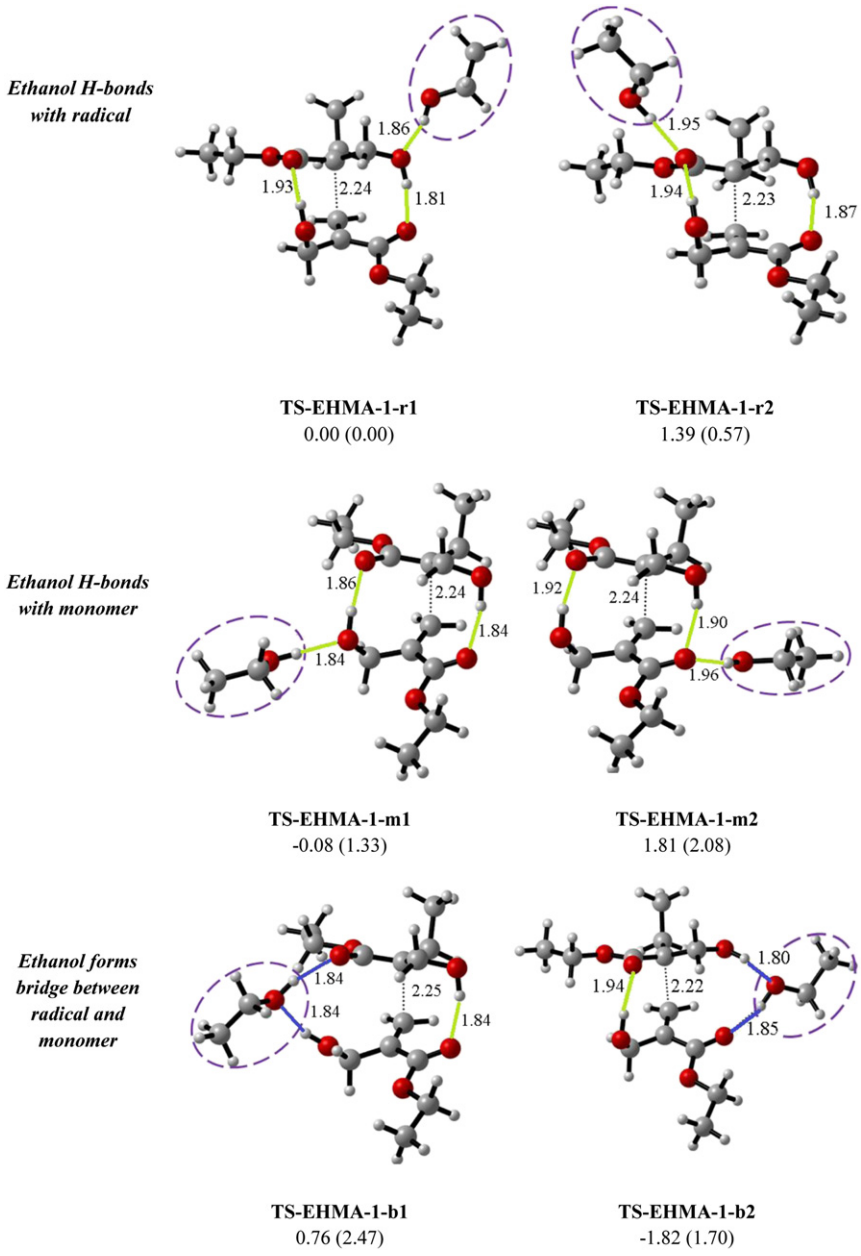


**Fig. 5.** Structures and relative Gibbs free energies (BSSE corrections included) of the transition state–solvent complexes of EHMA. IEF-PCM ($\varepsilon = 24.85$ for ethanol) calculations in parenthesis. MPW1K/6-311 + G(3df,2p)//B3LYP/6-31 + G(d). Green bonds: intermolecular H-bonding and ethanol H-bonds to monomer or radical, blue bonds show bridging H-bonds. (For interpretation of the references to color in this figure legend, the reader is referred to the web version of this article.)

### 3.3. Comparison of EMA and EHMA

Calculations in bulk (Table 4) show that $k_p$ values for EHMA are higher than those for EMA, most probably due to the hydrogen-bonds that stabilize the transition structures of EHMA. Davis *et al.* claim that [5] that regardless of solvent effect, $k_p$ of EHMA is more than 12–40 % higher than $k_p$ of EMA. Thus considering the $k_p$ of EMA as measured by Zammit *et al.* [4] in bulk together with the measurements of Davis *et al.* for EHMA, yields a $k_{p(EMA)}/k_{p(EHMA)}$ ratio of 0.35 Note that, Davis *et al.* expect $k_p$ of EHMA in bulk to be higher than the one in ethanol, so the $k_{p(EMA)}/k_{p(EHMA)}$ ratio should actually be lower than 0.35; thus experimental trend has been reproduced qualitatively with calculations. In the case of EHMA, due to the presence of intermolecular hydrogen-bonding, the propagating species are closer to each other and this facilitates the reaction.

### 3.4. EHMA polymerization in ethanol and toluene

For EHMA, the intermolecular hydrogen-bonded transition state structure geometry, **TS-EHMA-1** (syndiotactic) is the most stable one (Fig. 4). This structure has been used to calculate the $k_p$ values in toluene ($\varepsilon = 2.37$) and ethanol ($\varepsilon = 24.85$). The first two rows of Table 5 display the kinetic results with the continuum solvent model IEF-PCM where the two solvents toluene and ethanol, have been considered implicitly. The ratio of $k_p$'s in toluene and ethanol ($k_{p(toluene)}/k_{p(ethanol)}$) qualitatively reflects the experimental ratio (first row of Table 6) but is slightly higher than expected. Due to ethanol's hydrogen-bonding potential, an investigation of the role of explicit ethanol molecules in the polymerization of EHMA is therefore more than desirable. However, many hydrogen-bonding possibilities exist in the transition state; hydrogen-bond donor groups that are taken into account are the monomer and radical

hydroxyl groups; hydrogen-bond acceptors are the monomer and radical carbonyl groups. **TS-EHMA-1** was chosen for further explicit solvation by ethanol, since it represents the lowest energy transition structure.

To be able to calculate $k_p$ with explicit ethanol molecules, the optimum positions at which ethanol can hydrogen-bond to the monomer or/and the radical have been considered. As shown in Scheme 4, there are three H-bond acceptor oxygen atoms and one H-bond donor hydrogen atom in the monomer and the radical. Ethanol is also both a hydrogen-bond acceptor and donor, therefore, all possibilities were considered. As seen in Fig. 5, an ethanol bridging the radical and the monomer (**TS-EHMA-1-b1** and **TS-EHMA-1-b2**) does not further stabilize these structures since the bridging ethanol ruptures intermolecular hydrogen-bonds between the monomer and the radical, which seem to be preferred over hydrogen-bonds with ethanol. After optimizing the complexes, the supermolecule is further immersed in a continuum solvent environment; $k_p$ is calculated to see the effect of both explicit and implicit solvent on the propagation rate constant (Table 5). Since the relative Gibbs free energy differences of the transition states are rather small, all combinations have been considered and the weighted average of Gibbs free energies of activation for all transition states with explicit ethanol molecules have been taken into account. The ratio of $k_{p(toluene)}/k_{p(ethanol)}$ with explicit/implicit ethanol and implicit toluene is tabulated in Table 6.

Experimentally one notices some decrease in $k_p$ upon dilution with ethanol (Table 1). The more ethanol molecules are present in the reactive media, the larger the disruptive effect of ethanol in rupturing or weakening the intermolecular H-bonds between the monomer and the radical, which results in a slight decrease of the reaction rate. On the other hand, the opposite is observed with toluene as solvent; the propagation rate $k_p$ increases with increasing amount of toluene. This is entirely consistent with the idea that toluene cannot interrupt favorable hydrogen-bonds between the monomer and the radical in the transition state, the propagating species are closer to each other when surrounded by hydrophobic toluene molecules and the rate increases. The slightly larger propagation rate for toluene is well described by the calculations (Table 6). On the quantitative level the experimental ratio of 2.40 (Table 1) is even correctly reproduced if the ethanol solvent molecules are explicitly taken into consideration.

As already mentioned by Beuermann [32], Buback [33] and Radom [34] the effect of the solvent on the Arrhenius parameters - pre-exponential factor, $A$ and activation energy, $E_a$ - is of uttermost importance in order to rationalize the origins of the solvent effect. Table 7 displays the calculated (MPW1K/6-311 + G(3df,2p)//B3LYP/6-31 + G(d)) Arrhenius parameters of the free radical polymerization of EHMA in toluene and ethanol. The experimental Arrhenius parameters reported in Table 1 for EHMA in toluene (1:3) and ethanol (1:3) show that the 2.40 fold rate acceleration in toluene is partially dependent on the activation barrier (1.44 fold) but mainly due to the frequency factor (1.67 fold). The calculated Arrhenius parameters for ethanol and toluene show that the pre-exponential factor is mainly responsible for the rate acceleration in toluene (2.29 fold) as compared to the one in ethanol. In toluene, the EHMA monomers are stabilized by intramolecular H-bonding and tend to form 6-membered rings as displayed in Fig. 3 or they can make H-bonds with each other. Toluene is not expected to significantly alter the orientation of EHMA molecules whereas in ethanol these species will tend to form hydrogen-bonds with the solvent and lose their ordered aggregation patterns. As a result, the reactants will tend to be less ordered in ethanol. The transition structures in both media being more or less equally disordered the difference in entropy (disorder) between the transition structures and the reactants are expected to be smaller in ethanol. Thus the frequency factor which is measure of disorder between the transition structure and the reactants is expected to be higher in toluene. Our calculations attribute the 2.28 fold rate increase in toluene mainly to an increase in the frequency factor. This finding is slightly overestimated in the calculations as compared to experiment probably due to the small dimeric size of the model chosen as compared to the propagating long chain.

**Table 7**
Kinetic parameters for EHMA in different media at 303 K[a]

| | $E_a$ (kcal mol$^{-1}$) | $A$ ($10^4$ L mol$^{-1}$ s$^{-1}$) | $k_p$ (L mol$^{-1}$ s$^{-1}$) |
|---|---|---|---|
| Toluene[b] | 5.82 | 18.2 | 11.54 |
| Ethanol[c] | 5.78 | 7.42 | 5.03 |

[a] (MPW1K/6-311 + G(3df,2p)//B3LYP/6-31 + G(d)).
[b] TS-EHMA-1.
[c] weighted average values for the structures in Fig. 5.

## 4. Conclusion

In this study, the free radical polymerization (FRP) behavior of EHMA in bulk, ethanol and toluene has been modeled and compared to the FRP of EMA in bulk. In agreement with experiment, the FRP of EHMA is found to be slightly accelerated in toluene as compared to ethanol. Ethanol can explicitly interact with the propagating EHMA monomers, destroying their regular 6-membered ring shape via hydrogen-bonding. The solvent ethanol destroys the order of the reactants, decreasing the entropy of activation as compared to the same reaction in hydrophobic toluene. These results explain the experimentally observed dilution effects with both solvents: dilution with ethanol decelerates the reaction – due to the disruptive effect of ethanol – whereas dilution with toluene accelerates the reaction because of the hydrophobic nature of the solvent. EMA, which is known to have a slightly smaller gel effect than MMA, is commercially used in bulk and its polymerization behavior has been compared to the one of EHMA. Calculations predict the qualitative rate accelerating behavior of EHMA as compared to the EMA and reproduce qualitatively the experimental trend justifying the usage of the dimeric models proposed in this study for further qualitative understanding of the relative free radical polymerization behavior of acrylate derivatives.

## Acknowledgments

Computing resources used in this work were provided by the National Center for High Performance Computing of Turkey (UYBHM) under grant number 1001322011. The UGent authors thank the FWO (Fonds voor Wetenschappelijk Onderzoek - Vlaanderen, Fund for Scientific Research – Flanders), the research board of Ghent University for the bilateral project Ghent – Istanbul and the IAP-BELSPO project in the frame of IAP 6/27 for financial support of this research. B.D. would like to thank Dr. Isa Degirmenci for his suggestions and comments.

## References

[1] (a) Odian G. Principles of polymerization. New York: Wiley-Interscience; 1991;
(b) Satoh K, Kamigatio M. Chem Rev 2009;109:5120–56.
[2] De Sterck B, Vaneerdeweg F, Du Prez F, Waroquier M, Van Speybroeck V. Macromolecules 2010;43:827–36.
[3] (a) Kloosterboer JG. Adv Polym Sci 1988;84:1–61;
(b) Decker C. Prog Polym Sci 1996;21:593–650;
(c) Anseth KS, Newman SM, Bowman CN. Adv Polym Sci 1995;122:177–217.
[4] Zammit MD, Coote ML, Davis TP, Willet GD. Macromolecules 1998;31:955–63.

[5] Morrison DA, Davis TP. Macromol Chem Phys 2000;201:2128–37.
[6] (a) Beuermann S, Nelke D. Macromol Chem Phys 2003;204:460–70;
(b) Beuermann S, García N. Macromolecules 2004;37:3018–25.
[7] (a) Degirmenci I, Avci D, Aviyente V, Van Cauter K, Van Speybroeck V, Waroquier M. Macromolecules 2007;40:9580–602;
(b) Degirmenci I, Aviyente V, Van Speybroeck V, Waroquier M. Macromolecules 2009;42:3033–41.
[8] (a) Karahan O, Avci D, Aviyente V. J Polym Sci Part A Polym Chem 2011;49:3058–68;
(b) Gunaydin H, Seyhan S, Senyurt Tuzun N, Avci D, Aviyente V. Int J Quantum Chem 2005;103:176–89.
[9] (a) Ueda M, Koyama T, Mano M, Yazawa M. J Polym Sci Part A Polym Chem Ed 1989;27:751–62;
(b) Avci D, Kusefoglu SH. J Polym Sci Part A Polym Chem 1993;31:2941–9;
(c) Avci D, Kusefoglu SH, Thompson RD, Mathias LJ. J Polym Sci Part A Polym Chem 1994;32:2937–45.
[10] (a) Smith TJ, Shemper BS, Nobles JS, Casanova AM, Ott C, Mathias LJ. Polymer 2003;44:6211–6;
(b) Avcı D. Private communications; 2006.
[11] Antonucci JM, Fowler BO, Weir MD, Sktrtic D, Stansbury JW. J Mater Sci Mater Med 2008;19:3263–71.
[12] Rodríguez RC, Bordegé V, Sánchez-Chaves M, Fernández-García M. J Polym Sci Part A Polym Chem 2006;44:5618–29.
[13] Davis TP, Zammit MD, Heuts JP, Moody K. ChemComm 1998;31:2383–4.
[14] (a) Blaker JW. US Patent 4,752,123; 1988.
(b) Larsen HO. US Patent 4,495,313; 1985.
[15] (a) Kilambi H, Stansbury JW, Bowman CN. Macromolecules 2007;40:47–54;
(b) Lee TY, Roper TM, Jönsson ES, Guymon CA, Hoyle CE. Macromolecules 2004;37:3659–65;
(c) Jansen JFGA, Dias AA, Dorschu M, Coussens B. Macromolecules 2003;36:3861–73;
(d) Lemon MT, Jones MS, Stansbury JW. J Biomed Mater Res Part A 2007;83A(3):734–46.
[16] (a) Holmes RG, Rueggeberg FA, Callan RS, Caughman F, Chan DCN, Pashley DH, et al. Dent Mater 2007;23:1506–12;
(b) Hirano T, Kamikubo T, Fujioka Y, Sato T. Eur Polym J 2008;44:1053–9;
(c) Valdebenito A, Encinas MV. Polym Int 2010;59:1246–51.
[17] Beuermann S. Macromol Rapid Commun 2009;30:1066–88.
[18] Frisch MJTGW, Schlegel HB, Scuseria GE, Robb MA, Cheeseman JR, Montgomery Jr JA, et al. Gaussian 03. Revision D.01. Wallingford CT: Gaussian. Inc; 2004. Gaussian. Inc. Wallingford CT, 2004.
[19] Frisch MJ, Trucks GW, Schlegel HB, Scuseria GE, Robb MA, Cheeseman JR, et al. Gaussian 09. Wallingford CT: Gaussian, Inc.; 2009.
[20] (a) Becke AD. Phys ReV A 1988;38:3098–100;
(b) Lee C, Yang W, Parr RG. Phys ReV B 1988;37:785–9;
(c) Becke AD. J Chem Phys 1993;98:5648–56.
[21] Boese AD, Martin JML. J Chem Phys 2004;121:3405–16.
[22] Lynch BJ, Fast PL, Harris M, Truhlar DG. J Phys Chem A 2000;104:4811–5.
[23] (a) Truhlar DG, Hase WL, Hynes JT. J Phys Chem 1983;87:2664–82;
(b) Laidler KJ, King MC. J Phys Chem 1983;87:2657–64;
(c) Pechukas P. Annu Rev Phys Chem 1981;32:159–77;
(d) Pechukas P. Ber Bunsen-Ges Phys Chem 1982;86:372;
(e) Truhlar DG, Garrett BC, Klippenstein SC. J Phys Chem 1996;100:12771–800.
[24] (a) Tomasi J, Mennucci B, Cance's E. J Mol Struc-Theochem 1999;464:211–26;
(b) Cance's MT, Mennucci B, Tomasi J. J Chem Phys 1997;107:3032–41;
(c) Mennucci B, Tomasi J. J Chem Phys 1997;106:5151–8;
(d) Mennucci B, Cancès E, Tomasi J. J Phys Chem B 1997;101:10506–17.
[25] Barone V, Cossi M. J Phys Chem A 1998;102:1995–2001.
[26] (a) Pliego JR, Riveros JM. J Phys Chem A 2001;105:7241e7;
(b) Kelly CP, Cramer CJ, Truhlar DG. J Phys Chem A 2006;110:2493e9.
[27] Jansen HB, Ros P. Chem Phys Lett 1969;3:140–3.
[28] Liptak MD, Gross KC, Seybold PG, Feldgus S, Shields GC. J Am Chem Soc 2002;124:6421–7.
[29] Van Speybroeck V, Van Neck D, Wauters S, Saeys M, Marin GB. J Phys Chem A 2000;104:10939–50.
[30] Isobe Y, Yamada K, Nakano T, Okamoto Y. Macromolecules 1999;32:5979–81.
[31] Merrick JP, Moran D, Radom L. J Phys Chem A 2007;111:11683–700.
[32] Beurmann S, Buback M, Hesse P, Lacik I. Macromolecules 2006;39:184–93.
[33] Buback M. Macromol Symp 2009;275:90–101.
[34] Johan PA, Gilbert RG, Radom L. Macromolecules 1995;28:8771–81.